

WAVE AND RAY ANALYSIS OF A TYPE OF CLOAK EXHIBITING MAGNIFIED AND SHIFTED SCATTERING EFFECT

Y. Luo, J.-J. Zhang, and H.-S. Chen

The Electromagnetics Academy at Zhejiang University
Zhejiang University
Hangzhou 310027, China

B.-I. Wu

Research Laboratory of Electronics
Massachusetts Institute of Technology
Cambridge, Massachusetts 02139, USA

L.-X. Ran

Department of Information and Electronics Engineering
Zhejiang University
Hangzhou 310027, China

Abstract—Ray-tracing exercise and full-wave analysis were performed to validate the performance of a type of cloak composed of isotropic metamaterials. It is shown that objects inside the ‘folded region’ of this cloak appear invisible to the incoming light from a ray tracing exercise, but exhibit magnified and shifted scattering under a plane wave illumination from a full wave analysis. Gaussian beams are introduced to resolve this interesting paradox resulted from these two methods. We show that at the time-harmonic state, small energy can be diffracted into the folded region and contribute to the resonant state even when the Gaussian beam is steered away from the cloak with an object inside. A scattering pattern identical to that scattered from the image of the object will be formed, which agrees well with the phenomenon in the plane wave incidence case.

Corresponding author: H.-S. Chen (hansomchen@zju.edu.cn).

1. INTRODUCTION

Cloaking an obstacle from electromagnetic wave (EM) detection has attracted much interest. To make an object invisible, we need to guarantee the scattering cross section of the object as small as possible. Alù and Engheta presented the technique of using plasmonic and metamaterial covers to reduce the total scattering of a single or a collection of subwavelength spheres [1, 2], which relies on an inherently nonresonant scattering cancellation phenomenon; In Ref. [3], a method of concealing polarizable lines or point dipoles situated near a cloak made of a superlens was suggested by Milton et al. [3]; Based on the form invariance of Maxwell's equations, Pendry et al. proposed the optical transformation approach to design invisibility cloak with zero scattering cross section [4]. This methodology has recently won much more concerns [5–17], since wave cannot penetrate into the core of the cloaking device and the cloak can effectively render object of any shape and size invisible.

Different from previous efforts which try to conceal an object by minimizing its scattering, we propose an inverse way to camouflage the object by magnifying and shifting the scattering from the obstacle so that it seems to be produced by a much larger scatterer deviated from its original position. The proposed cloak is based on the superimaging effect of left-handed medium (LHM) [18] coating and can be used to disguise the true nature of the object, e.g., the position, the size, etc, and further mislead the detector who uses the time-harmonic EM waves. However, ray approximation method predicts a different behavior, showing that light can be bent around the 'folded region' of the cloak, making the object inside invisible. Gaussian beam which has a flexibility to be modeled as a ray (i.e., narrow Gaussian beam) or a plane wave (i.e., wide Gaussian beam) is implemented to resolve this paradox. We show that at time-harmonic state, even if the narrow Gaussian beam (or ray) is shifted from the cloak, small energy can still be diffracted into the folded region, inducing the resonance inside. Therefore when an object is located inside the coating layer, a scattering pattern identical to that scattered from the image of the object will be formed under a time-harmonic wave incidence. Apart from the anomalous phenomenon brought about by this cloak, it is also worth mentioning that this type of cloak can be implemented by isotropic negative index materials with the magnitude of the spatially varying refractive index larger than one everywhere. In addition, the material parameters of the cloak do not have extreme value (zero or infinity) anywhere. Therefore, concealment can be achieved with artificially structured negative-index media (NIM) like

phonic crystal [19] or subwavelength dielectric resonator [20].

For simplification, we suppose the spherical cloaking shell is a shell with inner radius R_1 and outer radius R_2 . Under a radial mapping $r' = f(r)$, the material parameters of the three-dimensional (3D) transformation medium will take the form

$$\varepsilon_r = \mu_r = \frac{f^2(r)}{r^2 f'(r)}, \quad \varepsilon_\theta = \mu_\theta = \varepsilon_\varphi = \mu_\varphi = f'(r). \quad (1)$$

The invisibility property requires $f(R_1) = 0$. Under this condition, it can be easily concluded that the parameters are strongly anisotropic and the radial components are zero at the inner surface. In order to reduce the anisotropy of the cloak, we choose $f(r)$ to be $f_1(r) = R_2^2/r$, which is monotonically decreasing as depicted in Fig. 1(a) ($f(r) = r$ represents the free space in the outer region). The corresponding permittivity and permeability become $\varepsilon_1 = \mu_1 = -R_2^2/r^2$, which means the coating is constructed by spatially variant isotropic LHM and the magnitude of the parameters are all larger than 1 (since $R_1 < r < R_2$). In order to make the impedance of the inner core matched with that of the coating layer, we let the material in the inner core be a RHM with the parameters: $\varepsilon_2 = \mu_2 = (R_2/R_1)^2$. We can consider the LHM coating along with the RHM core as a whole concealing device, whose parameters can be achieved by a non-monotonic transformation function shown in Fig. 1(a). It should be noted that in the folded region $R_0 < r < R_2$, a certain value of $f(r)$ corresponds to two different radii. In fact, many interesting phenomena are correlated with that region, which will be addressed later.

The function of the cloak is first demonstrated by using a ray tracing exercise. By taking the geometry limit of Maxwell's equations, the light path of the ray can be obtained with numerical integration of a set of Hamilton's equations [4, 5]. The results are shown in Fig. 1(b). The light is incident from the bottom and propagating along z direction. For comparison, we have also included the ray tracing results when the light is incident onto Pendry's cloak, which is shown in Fig. 1(c). Different from Pendry's perfect cloak which guides the rays around the central volume, the cloak in Fig. 1(b) guides the light to penetrate the core, but bends it all around the aforementioned 'folded region'. Therefore, from the ray tracing analysis, the object located in the folded region, as shown in Fig. 1(b), is invisible to ray detection.

However, different phenomena can be observed under a full wave analysis. Suppose a linearly polarized plane wave with unit amplitude $E^{inc} = \hat{x}e^{ik_0z}$ is incident upon the coating along the z direction. As explained by Fig. 2, a perfect electric conducting (PEC) sphere with radius R_s is located at the position $\bar{r}_0 (r_0, \theta_0, \varphi_0)$ in the folded region

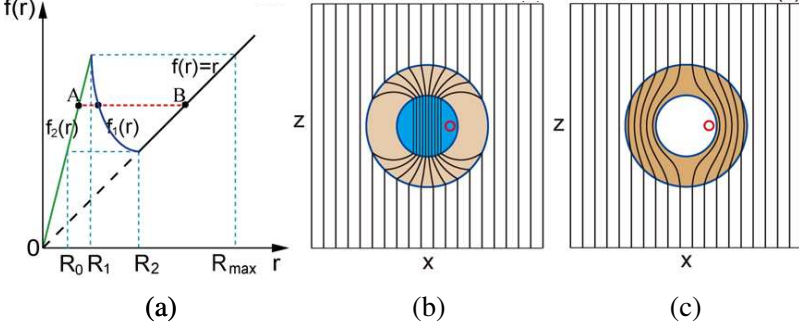


Figure 1. (a) Schematic figure of the functions $f(r)$ which is non-monotonic. The inner media ($0 < r < R_1$) is RHM, while the media in the coating ($R_1 < r < R_2$) is LHM. The fold ($R_0 < r < R_2$) indicates the hidden region. (b) Ray trajectories when the scatterer is located at the inner core. The light has been smoothly bent around this cloak. (c) The path of the rays when a scatterer is placed in an ideal transformation cloak proposed by Pendry. No light can enter into the center of the shell.

($R_0 < r < R_2$) of the coating. Here, \bar{r}_0 is a position vector whose three coordinate parameters are r_0, θ_0, φ_0 , respectively. We use Mie scattering theory to study this case [21]. Similar to the process in Ref. [10, 14, 22–26], by describing the fields with two Bromwich scalar potentials Φ_{TE} and Φ_{TM} and applying the boundary conditions, the scattered potentials can be obtained as:

$$\Phi_{\text{TE/TM}}^s = E_0 \sum_{n=1}^{\infty} \sum_{m=-n}^n \sum_{l=1}^{\infty} a_n T_n^{\text{TE/TM}} C_{n,m,l}^{\text{TE/TM}} \psi_n \left(k_0 r_0 \frac{R_2^2}{R_1^2} \right) \zeta_n(k_0 r) P_n^m(\cos \xi) e^{im(\varphi - \varphi_0)}, \quad (2)$$

where

$$\cos \xi = \cos \theta \cos \theta_0 + \sin \theta \sin \theta_0 \cos(\varphi - \varphi_0), \quad \text{and} \quad a_n = \frac{(-i)^{-n} (2n+1)}{n(n+1)}.$$

$$T_n^{\text{TM}} = -a_n \frac{\psi'_n \left[k_0 R_s (R_2/R_1)^2 \right]}{\zeta'_n \left[k_0 R_s (R_2/R_1)^2 \right]} \quad \text{and} \quad T_n^{\text{TE}} = -a_n \frac{\psi_n \left[k_0 R_s (R_2/R_1)^2 \right]}{\zeta_n \left[k_0 R_s (R_2/R_1)^2 \right]}$$

are the scattering coefficients. And $C_{n,m,l}^{\text{TE/TM}}$ is a definite expansion

coefficient [21]. ψ_n and ζ_n represent the Riccati-Bessel function of the first and the third kind, respectively. P_n^m is the n -th orders of the associated Legendre polynomials of degree m . It is worth mentioning that Eq. (2) is nonconvergent in the annulus region $R_2 < r < (R_2/R_1)^2 r_0$ due to the negative index of the material in the region $R_1 < r < R_2$, similar to the perfect lens imaging case in principle [27, 28]. In the domain $r > (R_2/R_1)^2 r_0$, Eq. (2) can be written in the following closed forms:

$$\begin{cases} \Phi_{\text{TM}}^s = \frac{\cos \varphi'}{\omega} \sum_{n=1}^{\infty} a_n T_n^{\text{TM}} \zeta_n \left(k_0 \left| \bar{r} - (R_2/R_1)^2 \bar{r}_0 \right| \right) P_n^1(\cos \theta') \\ \Phi_{\text{TE}}^s = \frac{\sin \varphi'}{\omega \eta_0} \sum_{n=1}^{\infty} a_n T_n^{\text{TE}} \zeta_n \left(k_0 \left| \bar{r} - (R_2/R_1)^2 \bar{r}_0 \right| \right) P_n^1(\cos \theta') \end{cases}, \quad (3)$$

where $\bar{r}'(r', \theta', \varphi') = \bar{r} - (R_2/R_1)^2 \bar{r}_0$ is a definite position vector (shown in Fig. 2). Eq. (3) shows that the scalar potentials of the whole system is exactly the same as that of a PEC sphere with radius $R_s(R_2/R_1)^2$ located at a position $(R_2/R_1)^2 \bar{r}_0$. Fig. 3(a) depicts the total field distribution of such case obtained by full wave analysis, where the frequency of the incident plane wave is 2 GHz. The radii of the inner and outer boundaries of the coating are 5 cm and 10 cm respectively, and a PEC sphere with the radius $R_s = 1.5$ cm is located at Point A (corresponding to Point A in Fig. 1(a)) inside the cloak. A magnified image is formed at Point B (corresponding to Point B in Fig. 1(a)). Fig. 3(b) displays the case where a conductive sphere with radius 6 cm

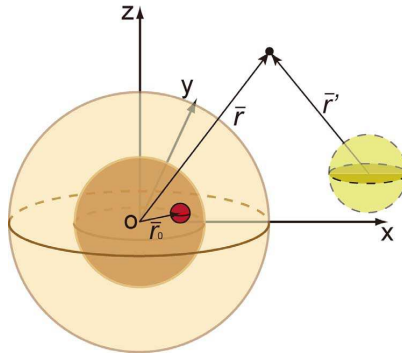


Figure 2. (a) 3D geometry of an obstacle (red solid object) with a radius $R_s = 1.5$ cm located inside the cloak at the position $\bar{r}_0(r_0, \theta_0, \varphi_0)$. The transparent red object with dashed contour stands for the image which will be formed under an EM wave illumination.

is placed at Point B in free space. By comparison, we find that the field distributions in the two cases are identical, indicating that an observers outside will ‘see’ a bigger scatterer (with a size magnification of 4 in this case) which has been shifted from its real position. In this way, both the volume and position information of the object will be disguised, misleading the observer effectively. This interesting phenomenon can be understood by checking Fig. 1(a) again. Note that at Point A and Point B , $f(r)$ have the same value, indicating that an object at Point A of the cloaking device will cause the identical scattering to that from a larger object (with a size magnification of $(R_2/R_1)^2$) located at Point B in free space ($r > R_2$). One thing worth pointing out is that, it takes some time for the field distribution shown in Fig. 3(a) to be established. In fact, under the outer illumination, the coating will concentrate the incoming wave into the internal region before reaching the steady state. During this period, the whole system will store energy from the incident wave, making some energy circulate in the folded region. Thanks to this energy circulation, the scattering shift and enhancement phenomena are gradually formed in the time harmonic state. When the obstacle inside the cloak is absent, as shown in Fig. 3(c), the energy is still circulating in the folded region without introducing any scattering. In addition, by choosing a different transformation function, the image of the scatterer can be located at a much greater distance from its original position. For example, in our above analysis, $f(R_1) = R_2^2/R_1$, if we choose f with $f(R_1) = C$ where C is much larger than R_2^2/R_1 , we will see a magnification of C/R_1 , and a much larger distance between the imaging and the object. In this case, the disguising effect will be more effective. The only cost is that the coating material will be anisotropic.

The results of the ray tracing method and the full wave analysis method are seemingly inconsistent. The paradox comes from the fact that the ray tracing method has not considered the diffraction of the light into the folded region. In order to further understand this phenomenon from physical perspective, we consider the case where a Gaussian beam is incident upon the cloak in the free space. The fields of the incident beam can be decomposed into TE and TM modes as

$$\Phi_{T/TM}^i = E_0 \sum_{n=1}^{\infty} \sum_{m=-n}^n D_{n,p,w}^{TE/TM} g_{n,m}^{TE/TM} \psi_n(k_0 r) P_n^m(\cos \theta) e^{im\varphi} \quad (4)$$

where $D_{n,p,w}^{TE/TM}$ and $g_{n,m}^{TE/TM}$ are the expansion coefficients which can be determined through the approach of Ref. [29]. The scattered field can be deduced by solving the boundary equations. Suppose the inner and outer radius of the coating is $R_1 = 20\lambda$ and $R_2 = 40\lambda$, and the PEC obstacle with radius $R = 2\lambda$ is located at the folded region.

Note that here the wavelength is very small compared with the size of the cloak. Instead of achieving scattering shift and enhancement, the whole cloaking device compresses the incoming Gaussian beam and guide it around the folded region, as depicted in Fig. 4(a). In other words, the scattered field outside the cloak approaches to zero and the obstacle in the folded region shown in Fig. 4(a) is invisible to outer observers. This phenomenon of wave bending is similar to what we find in the ray tracing method, where all the waves incident upon the outer surface of the LHM coating have been concentrated in a small region ($r < R_0$, R_0 is shown in Fig. 1(a)) as they penetrate into the core. In plane wave incidence case, the power of the incident wave will diffract into the folded region surrounding the obstacle due to the high spatial dispersion. And the energy will be stored there and circulate between the LHM coating and the RHM core. This is also the reason why the power flows inside the core is larger than the power flows through the whole system [14]. However, in the cases where the spatial dispersion of the incident beam is so small that we can neglect the power dispersed into the cloak, the detecting beam will transmit through the cloak without touching the obstacle in the folded region. In order to observe the effect of the dispersed power more clearly, we remove the scatterer and move the Gaussian beam away from the cloak, and then calculate the field distribution inside and outside the cloak. Fig. 4(b) shows the field distribution obtained by analytical calculation. We can observe that in the steady state, a resonance is induced by the dispersed field and the power is circulated in the folded region. In fact, since the field

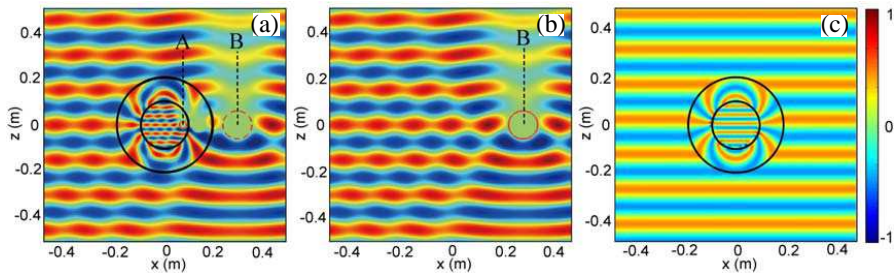


Figure 3. (a) Field distribution of an E_x polarized plane wave incident upon the coating along z direction when a conductive sphere with radius 1.5 cm is placed at the position A in the hidden region of coating. (b) Field distribution of the same plane wave incident upon a conductive sphere with radius 6 cm placed at the position B in free space. (c) Field distribution of the plane wave incident upon the coating when there are no scatterers inside the coating.

dispersed into the cloak is very weak, it takes quite a long time for this steady state to be established. Next, we replace the beam in Fig. 4(a) with a wide Gaussian beam, as shown in Fig. 4(c). It is found that, when the width of the Gaussian beam is comparable with the size of the cloak, very similar field distribution to that of the plane wave case (Fig. 3(a)) is formed. Similarly, we also change the Gaussian beam in Fig. 4(b) for a wide beam, which is shown in Fig. 4(d). The same as in Fig. 3(c), the wave is concentrated in the center of the cloak.

The above analysis help us better understand the seemingly contradiction between the ray tracing and full-wave methods. The

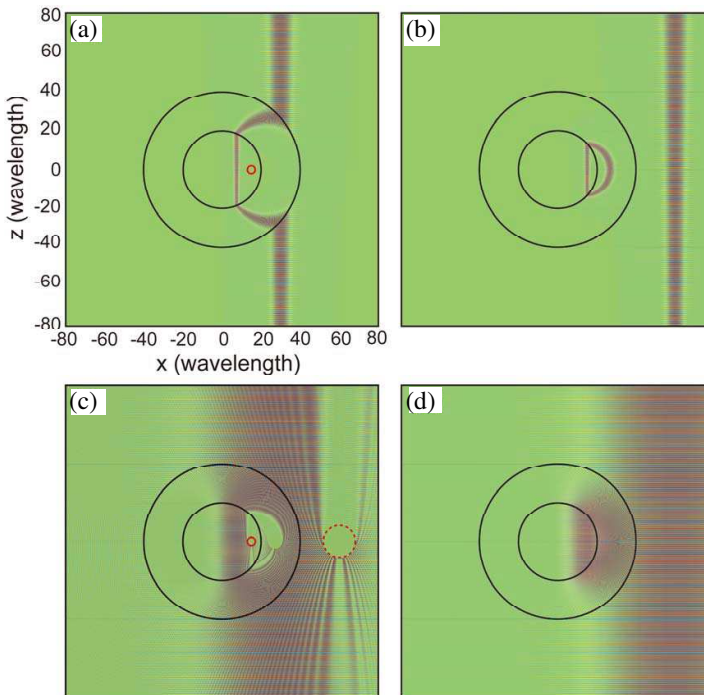


Figure 4. (a) Snapshot of the electric field distribution when a narrow Gaussian beam is incident upon the cloak with $R_2 = 40\lambda$ and $R_1 = 20\lambda$ along the z direction. A PEC scatterer is located inside the folded region of the cloak. (b) The electric field distribution when a narrow Gaussian beam is shifted away from the cloak. A resonance can be observed inside the folded region, which is due to the accumulation of the dispersed field from the Gaussian beam. (c) Similar to case (a), but incident with a wide Gaussian beam. (d) Similar to case (b), but incident with a wide Gaussian beam.

narrow Gaussian beam analysis shows high agreement with the ray tracing exercise in most of the cases, where the beam incident upon the cloak will all be bent around the folded region without causing scattering. However, different from what we find from the ray tracing method, a narrow Gaussian beam passing by the cloak will cause an inherent resonance of the cloak as long as the time is long enough. Therefore, the resonances of the ray in the negative refractive index media need to be included in the ray tracing model in order to solve this paradox. Similar contradiction of the ray and wave analysis can also be shown in a configuration of negative space composed of negative refractive index materials [18]. In our case we use the narrow Gaussian beam, which can be vividly viewed as a ray, as shown in Fig. 4(b), and we can find the internal resonance of the ray in the interface of the positive and negative index materials. The enhanced scattering has also been numerically analyzed and was pointed out as a superscattering effect in [30] with the object located in the center of the cloak, which is specific case of our paper. The 3D configuration is also different with the 2D cylindrical superlens [31] and the planar superlens [3], although all of them are based on multi-valued coordinate transformation [32]. In addition, we analyze the scattering properties instead of imaging resolution [3, 31]. Since the total field is a combination of the incident field and an imaging of the field scattered from the object in the core, the phenomena can be interpreted as a focusing effect followed by destructive interference of the two fields. That is the reason why there is no object located in the imaging position but we can see a scattering field as if the field is scattered from the imaging point.

Another point worth noting is that the whole cloak is constructed by isotropic media. In geometric optics limit, the effective refraction index is the main factor we consider which can affect the light paths. It is required that the refraction index of the LH coating and the RH core are $n_1 = -R_2^2/r^2$ and $n_2 = (R_2/R_1)^2$ respectively (these parameters are also applicable to two dimensional cylindrical case), which is physically realizable with metamaterials, such as photonic crystal [19] and high dielectric resonators [20]. The reflection at the interfaces can be suppressed by controlling the thickness and surface termination of the LHM coating layer.

2. CONCLUSION

In summary, analytical full wave theory and ray tracing method have been introduced to examine the behavior of a type of cloak consisting of a spherical LHM coating and an RHM core. It is demonstrated that

this cloak will lead to a scattering enhancement instead of scattering reduction in contrast to all the traditional cloaks; the scattered field distribution can also be changed as if the scatterer is moved away from its original position. Thanks to those capabilities, the proposed cloak can be used to disguise the true information of the object, and further mislead the observer. Our approach provides a different perspective to achieve camouflage, and is an alternative to the published invisibility cloaking methods.

ACKNOWLEDGMENT

This work is sponsored by the National Science Foundation of China under grants 60801005 and 60531020, in part by the Zhejiang National Science Foundation under grant R1080320 and Y1080715 the Foundation for the Author of National Excellent Doctoral Dissertation of PR China under Grant No. 200950, the Ph.D Programs Foundation of MEC (No. 20070335120 and 200803351025), the NCET-07-0750, 863 Project (No. 2009AA01Z227), the Office of Naval Research (ONR) under contract N00014-06-1-0001, and the Department of the Air Force under Air Force contract FA8721-05-C-0002.

REFERENCES

1. Alù, A. and N. Engheta, "Achieving transparency with plasmonic and metamaterial coatings," *Phys. Rev. E*, Vol. 72, 016623, 2005.
2. Alù, A. and N. Engheta, "Multifrequency optical invisibility cloak with layered plasmonic shells," *Phys. Rev. Lett.*, Vol. 100, 113901, 2008.
3. Milton, G. W. and N. A. P. Nicorovici, "On the cloaking effects associated with anomalous localized resonance," *Proc. R. Soc. A*, Vol. 462, 3027–3059, 2006.
4. Pendry, J. B., D. Schurig, and D. R. Smith, "Controlling electromagnetic fields," *Science*, Vol. 312, 1780–1782, 2006.
5. Leonhardt, U., "Optical conformal mapping," *Science*, Vol. 312, 1777–1780, 2006.
6. Greenleaf, A., M. Lassas, and G. Uhlmann, "Anisotropic conductivities that cannot be detected by EIT," *Physiol. Meas.*, Vol. 24, 413–419, 2003.
7. Schurig, D., J. J. Mock, B. J. Justice, S. A. Cummer, J. B. Pendry, A. F. Starr, and D. R. Smith, "Metamaterial electromagnetic cloak at microwave frequencies," *Science*, Vol. 314, 977–980, 2006.

8. Cummer, S. A., B.-I. Popa, D. Schurig, D. R. Smith, and J. B. Pendry, "Full-wave simulations of electromagnetic cloaking structures," *Phys. Rev. E*, Vol. 74, 036621, 2006.
9. Greenleaf, A., Y. Kurylev, M. Lassas, and G. Uhlmann, "Improvement of cylindrical cloaking with the SHS lining," *Opt. Express*, Vol. 15, 12717–12734, 2007.
10. Chen, H., B.-I. Wu, B. Zhang, and J. A. Kong, "Electromagnetic wave interactions with metamaterial cloak," *Phys. Rev. Letts.*, Vol. 99, 063903, 2007.
11. Cai, W., U. K. Chettiar, A. V. Kildishev, and V. M. Shalaev, "Optical cloaking with metamaterials," *Nature Photon.*, Vol. 1, 224–227, 2007.
12. Weder, R., "A rigorous analysis of high-order electromagnetic invisibility cloaks," *J. Phys. A: Math. Theor.*, Vol. 41, 065207, 2008.
13. Zhang, J., J. Huangfu, Y. Luo, H. Chen, J. A. Kong, and B.-I. Wu, "Cloak for multilayered and gradually changing media," *Phys. Rev. B*, Vol. 77, 035116, 2008.
14. Luo, Y., H. Chen, J. Zhang, L. Ran, and J. A. Kong, "Design and analytical full-wave validation of the invisibility cloaks, concentrators, and field rotators created with a general class of transformations," *Phys. Rev. B*, Vol. 77, 125127, 2008.
15. Zhang, J. J., Y. Luo, S. Xi, H. Chen, L.-X. Ran, B.-I. Wu, and J. A. Kong, "Directive emission obtained by coordinate transformation," *Progress In Electromagnetics Research*, PIER 81, 437–446, 2008.
16. Zhang, J. J., Y. Luo, H. Chen, and B.-I. Wu, "Sensitivity of transformation cloak in engineering," *Progress In Electromagnetics Research*, PIER 84, 93–104, 2008.
17. Rahm, M., S. A. Cummer, D. Schurig, J. B. Pendry, and D. R. Smith, "Optical design of reflectionless complex media by finite embedded coordinate transformations," *Phys. Rev. Letts.*, Vol. 100, 063903, 2008.
18. Pendry, J. B. and D. R. Smith, "Reversing light with negative refraction," *Phys. Today*, Vol. 57, 37–43, 2004.
19. Rockstuhl, C., F. Lederer, C. Etrich, T. Pertsch, and T. Scharf, "Design of an artificial three-dimensional composite metamaterial with magnetic resonances in the visible range of the electromagnetic spectrum," *Phys. Rev. Letts.*, Vol. 99, 017401, 2007.
20. Schuller, J. A., R. Zia, T. Taubner, and M. L. Brongersma,

- “Dielectric metamaterials based on electric and magnetic resonances of silicon carbide particles,” *Phys. Rev. Letts.*, Vol. 99, 107401, 2007.
21. Balanis, C. A., *Advanced Engineering Electromagnetics*, Wiley, New York, 1989.
 22. Choi, S. H., D. W. Seo, and N. H. Myung, “Scattering analysis of open-ended cavity with inner object,” *Journal of Electromagnetic Waves and Applications*, Vol. 21, No. 12, 1689–1702, 2007.
 23. Li, Y. L., J. Y. Huang, and M. J. Wang, “Scattering cross section for airborne and its application,” *Journal of Electromagnetic Waves and Applications*, Vol. 21, No. 15, 2341–2349, 2007.
 24. Du, P., B. Z. Wang, H. Li, and G. Zheng, “Scattering analysis of large-scale periodic structures using the sub-entire domain basis function method and characteristic function method,” *Journal of Electromagnetic Waves and Applications*, Vol. 21, No. 14, 2085–2094, 2007.
 25. Abd-El-Raouf, H. and R. Mittra, “Scattering analysis of dielectric coated cones,” *Journal of Electromagnetic Waves and Applications*, Vol. 21, No. 13, 1857–1871, 2007.
 26. Xi, S., H. Chen, B. I. Wu, B. Zhang, J. Huangfu, D. Wang, and J. A. Kong, “Effects of different transformations on the performance of cylindrical cloaks,” *Journal of Electromagnetic Waves and Applications*, Vol. 22, No. 11–12, 1489–1497, 2008.
 27. Pendry, J. B., “Negative refraction makes a perfect lens,” *Phys. Rev. Letts.*, Vol. 85, 3966–3969, 2000.
 28. Pendry, J. B., “Negative refraction,” *Contemp. Phys.*, Vol. 45, 191–202, 2004.
 29. Han, Y. and Z. Wu, “Scattering of a spheroidal particle illuminated by a gaussian beam,” *Appl. Opt.*, Vol. 27, 2501–2509, 1988.
 30. Yang, T., H. Chen, X. Luo, and H. Ma, “Superscatterer: Enhancement of scattering with complementary media,” *Opt. Express*, Vol. 16, 18545–18550, 2008.
 31. Yan, M., W. Yan, and M. Qiu, “Cylindrical superlens by a coordinate transformation,” *Phys. Rev. B*, Vol. 78, 125113, 2008.
 32. Leonhardt, U. and T. G. Philbin, “General relativity in electrical engineering,” *New J. Phys.*, Vol. 8, 247, 2006.